Zenith Sky Brightness and Color during the March 14, 2025 Total Lunar Eclipse

Jennifer Jean Birriel
Brayden Schwegman
Department of Engineering Sciences, Morehead State University, 150 University Boulevard, Morehead, KY 40351; j.birriel@ moreheadstate.edu; bjschwegman@moreheadstate.edu

Received March 11, 2026; revised June 22, 2026; accepted June 23, 2026

Abstract During a lunar eclipse, the night sky darkens as the moon enters the umbral region of the Earth's shadow. Due to the refraction of solar rays by Earth's atmosphere, the lunar surface is illuminated by red light even during totality. We suggest that sky brightness studies using filtered Sky Quality Meters (SQMs) might help inform atmospheric scattering models. We present observations of zenith sky brightness during the March 14, 2025, total lunar eclipse from Morehead, Kentucky. Data were collected using a set of SQMs fitted with red (R), green(G), blue (B), and clear or luminous (L) filters. During totality, zenith sky brightness viewed through the L band was 19.0 ± 0.1 mag/arcsec^2 (in SQM magnitudes), in agreement with previous measurements made at this site during the January 19, 2019, lunar eclipse. The B–G color index shows little observable difference between B and G bandpasses. The B–R color index increases by 0.30 ± 0.14 mag/arcsec^2 during totality vs post totality, indicating a "reddening" of zenith sky color during totality. This is consistent with the red appearance of the Moon during totality.

1. Introduction

Scientific interest in lunar eclipses in modern times is largely focused on probing Earth's atmosphere (e.g. Gedzelman and Voller 2008; Muñoz and Pallé 2011; Di Giovanni 2018). Photometric and spectroscopic measurements of lunar surface brightness during totality can provide information regarding atmospheric properties including transparency, aerosol and ozone content, and atmospheric extinction of solar radiation.

The Dajon scale is a five-point scale to quantify the brightness of the eclipsed moon during totality (Espenak 2026). The scale runs from L = 0, a very dark moon that is barely visible, to L = 4, a very bright moon with a copper-red to orange color. The Danjon value should be assessed at mid-totality, as it is a measure of the depth of the moon in the umbral shadow. Factors affecting the Danjon index for a particular eclipse include the path of the moon through Earth's umbral shadow and atmospheric conditions (Yamaguchi 1978; Sigismondi 2019; Komitov and Kaftan 2022).

Lunar eclipses have been studied primarily from the point of view of lunar surface brightness. A small number of studies examine sky brightness during these events (e.g. Abousheli *et al.* 2023; Morton 1983; Dvorak 2005; Birriel and Adkins 2019; Birriel *et al.* 2020; Hernitschek *et al.* 2008; Góez Therán and Vargas Domínguez 2016, 2021); most of these studies examine the bolometric sky luminance. However, Morton (1983) examined light in the U, B, and V spectral bands in the region of the sky within a few degrees of the moon; his measurements were motivated by expected color changes due to the large amount of volcanic dust in the air.

The total solar eclipse of March 13–14, 2025, was visible throughout North America. We present photometric measurements in the L, R, G, B bands at a site in Morehead, Kentucky. At the observation location the eclipse lasted 6 hours and 3 minutes, with totality lasting 1 hour and 5 minutes. Skies were partly cloudy for several hours after sunset but cleared up at the start of the penumbra eclipse (P1) and remained clear for the entirety of the umbral portion of the eclipse. Visibility was approximated at 10 miles via archival data from timeanddate.com (Time and Date AS 1995–2026).

Spectrophotometric measurements of sky brightness might prove useful to inform scattering models such as those of Muñoz and Pallé (2011). Such measurements coupled with lunar images to ascertain the Danjon number could possibly be used to develop a relationship between Danjon numbers and zenith sky brightness measurements.

2. Instrumentation and observations

Zenith sky brightness measurements were obtained using a bank of four data-logging Sky Quality Meters (SQM-L-DL model) housed in a protective tubing, see Figure 1. Each SQM-L was equipped with one color filter, so the full set of four SQMs included a clear (L) filter, and a Red (R), Green (G), and Blue (B) filter (ZWO Astro 2026). The lens in the SQM-L models results in a 20-degree acceptance cone around zenith. Individual measurements are subject to an uncertainty of ± 0.1 magnitude per square arcsecond (mpsas), according to the manufacturer. Taking the difference between two different SQM measurements results in an experimental uncertainty

(a) (b)

Figure 1. (a) Bank of SQM-L-DL devices in weatherproof housing and mounted on a sawhorse viewed from the side. (b) A view from the top with filters visible, from left to right: Red (R), Green (G), Blue (B), and clear or luminous (L).

of ±0.14, using the addition of errors in quadrature. For full technical specifications and a report of SQM-L performance, readers are referred to Cinzano (2005).

Each SQM collected sky brightness data from sunset to sunrise from Morehead, Kentucky. SQM measurements must be corrected for transmission losses due to the glass window of the protective housing and the respective L, R, G, B filter transmission (see Figure 2). The transmission of each color filter is roughly uniform and approximately 92% along its bandpass. Our device was inspired by that of Spoelstra (2014) and we employ his method to determine our correction factors. The reading from each SQM depends on both the SQM detector response and the color filter transmission. The corrected brightness measured by each device is given by

$$m_{corrected} = m_{reading} - 2.5 \log (1 / R_{band}), \quad (1)$$

where R_{band} is the average response in the spectral band. This is determined by the sum of the detector response at each wavelength λ multiplied by the filter transmission T_{λ} in each wavelength interval Δλ and dividing by the number of wavelength intervals:

$$R_{band} = (\text{Sum} (R_{detector\ \lambda}\ T_{\lambda}) / n_{\Delta\lambda}. \quad (2)$$

The detector response, $R_{dectector\ \lambda}$, for the SQM was determined by Cinzaon 2005 (p. 6, Fig. 12). All correction factors are found in Table 1.

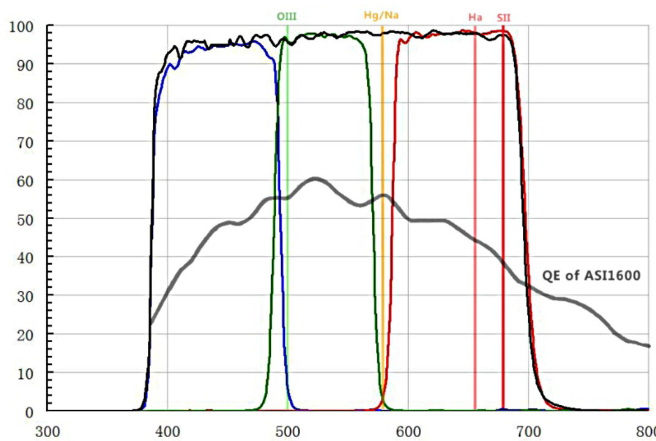

Figure 2. (Top) The transmission curves for the ZWO LRGB filter set (reprinted with permission, https://www.zwoastro.com/product/lrgb-filters). The black curve corresponds to the L of "luminous" filter. The R, G, B filters are represented by the red, green, and blue graphs, respectively. (Note: The grey curve is a quantum efficiency of the ZWO ASI1600 monochrome camera and is not relevant to this study as our detector is the Unihedron SQM-LE-DL.)

Table 1. Corrections for SQM response and RGB filter transmission.

Filter Color	*Wavelength Band (nm)*	*Center Wavelength (nm)*	*Correction Factors* R_{band} *(%)*	*Correction Factors* $-2.5 \log (1/R_{band})$ *(mag / arcsec²)*
Red	600–680	640	93	–0.08
Green	500–550	525	77	–0.29
Blue	411–470	440	59	–0.58

3. Results and discussion

Measurements of zenith sky brightness (in SQM magnitudes) were made from Morehead, Kentucky. Eclipse details for this site are found in Table 2. The evening started out with some passing clouds, but cleared as the penumbral eclipse began. Figure 3 displays the zenith sky brightness in all three bands. At maximum eclipse, zenith sky brightness in the L band was 19.0 ± 0.1 mag / arcsec^2. This value is consistent with measurements made at this site during the January 19, 2019, lunar eclipse and similar measurements made at this site during clear, new moon nights (19.3 ± 0.1 mag / arcsec^2).

Brightness measurements in the R, G, and B bands follow the general trends of the L band. The B and G band brightness measurements differ only slightly, see Figure 3. During totality

Table 2. Morehead, Kentucky (38.1841° N, 83.4351° W) eclipse characteristics.*

Eclipse Stage	*Local Time (EDT)*	*Lunar Altitude (°)*
P1: Penumbral eclipse begins	23:57	47.7
U1: Partial eclipse begins	01:09	53.7
U2: Total eclipse begins	02:26	52.7
Greatest eclipse	02:58	50.0
U3: Total eclipse ends	03:31	46.2
U4: Partial eclipse ends	04:47	34.4
P4: Penumbral eclipse ends	06:00	21.4

**Source timeanddate.com*

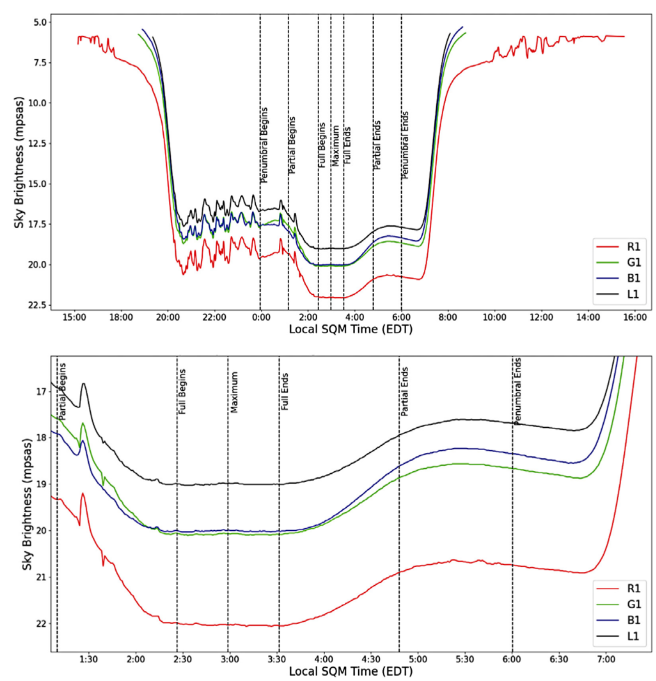

Figure 3. Total lunar eclipse adjusted zenith brightness vs time; Morehead, Kentucky (March 13–14, 2025). (Top) Zenith sky brightness recorded in SQM magnitudes by the L, R, G, B filtered SQMs from sunset to sunrise. The "jagged" nature of the data prior to the penumbral eclipse is due to passing clouds in the sky. All values are corrected for detector response and filter transmission. (Bottom) A close-up of the sky brightness excluding the cloudy, pre-eclipse sky.

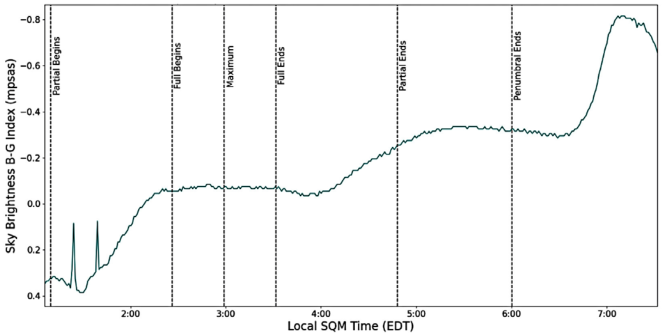

Figure 4. Total lunar eclipse adjusted blue–green index vs time; Morehead, Kentucky (March 13–14, 2025). The B–G index (in SQM magnitudes) during totality is estimated at 0.0 mpsas. It increases slightly after totality, in accordance with the 1/λ⁴ Rayleigh scattering relationship.

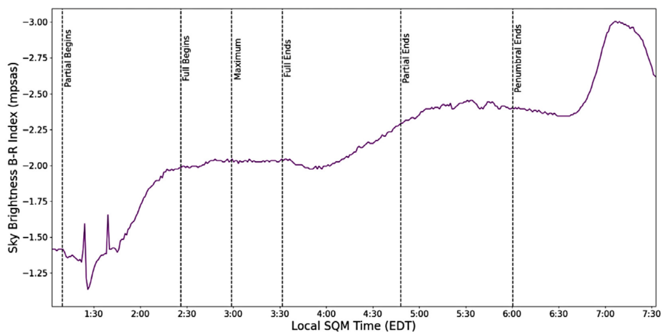

Figure 5. Total lunar eclipse adjusted blue–green index vs time; Morehead, Kentucky (March 13–14, 2025). The B–R color index (in SQM magnitudes) during totality is estimated at –2.00 mpsas while post totality, it is roughly –2.30 mpsas. Thus, during totality, zenith sky brightness is "redder" in accordance with the red lunar surface.

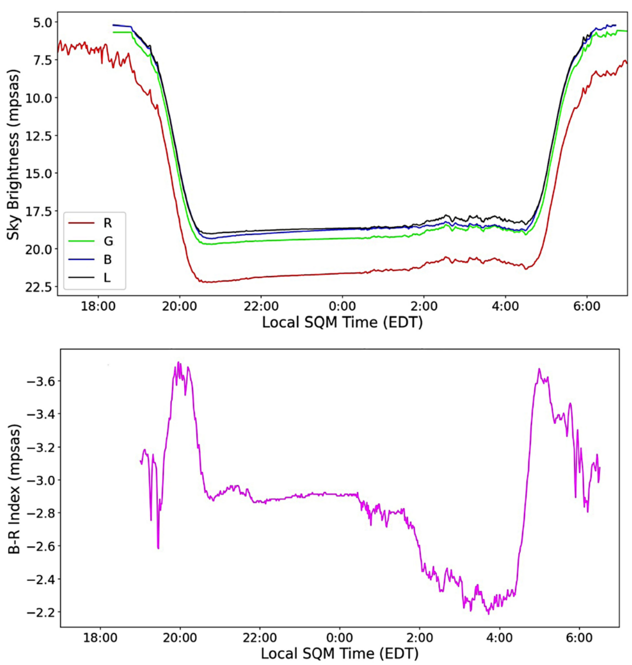

Figure 6. Zenith sky brightness (in SQM magnitudes) in the LRGB bands on a normal full moon night (May 1–2, 2026) in Morehead, Kentucky. The night was mainly clear but humidity increased from 47% for the first part of the night to just over 90% shortly after 1:00 A.M. (Bottom) The B–R color index is essentially constant at –2.9 mpsas, just prior to midnight, when the humidity is relatively constant. The observed decrease in color index from just after midnight until 4;30 A.M., is the result of steadily increasing humidity, resulting in greater scattering of blue light.

the B–G color index is essentially zero, and increases to -0.20 mag / arcsec² post-totality, as seen in Figure 4. The B–R color index is about –2.00 mag / arcsec² during totality compared to –2.30 mag / arcsec² post-totality. This corresponds to a difference of 0.30 mag / arcsec²: so the zenith sky is "redder" during totality. This reddening is consistent with the red appearance of the Moon during totality which results from both Rayleigh scattering and refraction by Earth's atmosphere.

For comparison, we obtained similar data on a normal full moon night at the same observation site. Data were collected with the same instrumentation on the night of May 1 to May 2, 2026. The night was mainly clear, however, humidity increased from 47% at 8:00 P.M. to 68% at 12:54 A.M. and subsequently increased to just over 90% by 3:00 A.M. (timeanddate.com). Note the constancy of zenith sky brightness prior to 12:54 A.M. followed by increasing brightness in every color band, as seen in Figure 6. High humidity leads to increased scattering of artificial light and, therefore, increased sky brightness (e.g. Kyba *et al.* 2011; Pramudya *et al.* 2019). The B–R index (Figure 6, bottom) becomes more positive as humidity increases in accordance with Rayleigh scattering. These data demonstrate that the B–R index at zenith, in the absence of large humidity changes, remains constant regardless of lunar altitude.

On the night of the March 13-14, 2025 total lunar eclipse, humidity at the observation location was nearly constant from 1:00 A.M. to 6:00 A.M. ranging from 58% to 64%. Therefore, the observed change in B–R index of +0.3 mag / arcsec² represnets a reddening of the zenith sky brightness during the lunar eclipse that results from terrestrial atmospheric refraction and Rayleigh scattering.

4. Conclusions

During a lunar eclipse, the surface of the moon remains visible throughout totality. The light reflected by the moon represents sunlight that is refracted, scattered, and attenuated by Earth's atmosphere (Cooper 2004). Spectrophotometric measurements of the night sky during such events can help inform models such as those of Muñoz and Pallé (2011). Using a standard device such as the SQM with a standard set of LRGB filters might prove useful as it would eliminate any differences between different instruments. Finally, it might be possible to correlate zenith sky color indices during totality with the Danjon index, similar to the proposed expression relating the Danjon index and the magnitude of the lunar surface during a total lunar eclipse (Di Giovanni 2018).

5. Acknowledgements

The authors wish to thank Morehead State University's Undergraduate Research Fellowship program for providing financial support. They also thank the anonymous referee for suggestions that improved the quality and clarity of this paper.

References

Aboushelib, M. F., Newar, S., Morcos, A. B., Shalabiea, O. M., and Awad. A. 2023, preprint (https://www.researchsquare.com/article/rs-3248504/v1).

Birriel, J. J., Adkins, J. K., Bertolo, A., Ehlert, R., McKeag, M., Ribas, S. J., and Tekaatch, A. 2020, *J. Amer. Assoc. Var. Star Obs.*, **48**, 76.

Birriel, J., and Adkins, J. K. 2019, *J. Amer. Assoc. Var. Star Obs.*, **47**, 94.

Cinzano, P. 2005, *ISTIL Internal Rep.*, No. 9, 1.4, 1.

Cooper, T. P. 2004, *Mon. Notes Astron. Soc. S. Afr.*, **63**, 60.

Di Giovanni, G. 2018, *J. Br. Astron. Assoc.*, **128**, 10.

Dvorak, S. 2005, *J. Amer. Assoc. Var. Star Obs.*, **34**, 72.

Espanek, F. , “NASA Eclipse Website: Danjon Scale of Lunar Eclipse Brightness” (https://eclipse.gsfc.nasa.gov/OH/Danjon.html).

Gedzelman, S. D., and Vollmer, M. 2008, *Appl. Opt.*, **47**, H149.

Góez Therán, C., and Vargas Domínguez, S. 2016, *Iranian J. Astron. Astrophys.*, **3**, 15.

Góez Therán, C., and Vargas Domínguez, S. 2021, *Rev. Mex. Astron. Astrofis.*, **57**, 57.

Hernitschek, N., Schmidt, E., and Vollmer, M. 2008, *Appl. Opt.*, **47**, H62.

Komitov, B. P. and Kaftan, V. I. 2022, *Geomagn. Aeron.*, **62**, 1117.

Kyba C. C. M., Ruhtz, T., Fischer, J., and Hölker, F., 2011, *PLoS ONE*, **6**, e17307 (https://doi.org/10.1371/journal.pone.0017307).

Morton, J. C. 1983, *Observatory*, **103**, 24.

Muñoz, A. G., and Pallé, E. 2011, *J. Quant. Spectrosc. Radiat. Transfer*, **112**, 1609.

Pramudya, Y., Budi, K. S., Okimustava, and Muchlas. 2019, *J. Phys.: Conf. Ser.*, **1231**, 012004.

Sigismondi, C. 2019, *Gerbertus*, **12**, 69.

Spoelstra, H. 2014, *J. Quant. Spectrosc. Radiat. Transfer*, **139**, 82.

Time and Date AS. 1995–2026, “timeanddate” (https://www.timeanddate.com).

Yamaguchi, M. 1978, *Irish Astron. J.*, **13**, 254.

ZWO Astro. 2026, "LRGB Filters" (https://www.zwoastro.com/product/lrgb-filters).